Field-effect resistance of gated graphitic polymeric ribbons: Numerical simulations

Alessandro Cresti,[1] Giuseppe Grosso,[1] and Giuseppe Pastori Parravicini[2]
[1]*NEST-CNR-INFM and Dipartimento di Fisica "E. Fermi," Università di Pisa, Largo Pontecorvo 3, I-56127 Pisa, Italy and CEA, LETI-Minatec, 17 rue des Martyrs, 38054 Grenoble Cedex 9, France*
[2]*NEST-CNR-INFM and Dipartimento di Fisica "A. Volta," Università di Pavia, Via A. Bassi 6, I-27100 Pavia, Italy*
(Received 14 May 2008; revised manuscript received 22 July 2008; published 26 September 2008)

We investigate the electronic and transport properties of undistorted gated polymers of the polyacene family by exploiting the tight-binding model for the system Hamiltonian and the nonequilibrium Keldysh formalism for charge transport. Our simulations reveal that, for smooth gate potentials varying only along the ribbon longitudinal axis, the electronic conductance as a function of the energy is quantized and presents crossover from conducting to insulating regimes. We interpret this behavior on the basis of the band structures entailed by the bipartite honeycomb topology of the lattice and the symmetry of the ribbons with even or odd number of chains (even-odd effect).

DOI: 10.1103/PhysRevB.78.115433 PACS number(s): 73.23.−b, 71.20.Rv, 73.21.Hb

I. INTRODUCTION

Organic nanostructures have gained enormous interest in the recent years as active materials for next generation molecular electronics.[1–4] A special effort has been dedicated to the understanding of the honeycomb arrangement of carbon atoms in olygomers, conjugated polymers, supramolecular structures, films, and more recently nanotubes[5] and graphene nanoribbons.[6] The above materials consist of the same aromatic carbons and are classified into two main structures according to their edge profile: "acene-edge type" (or zigzag edge type) and "phenanthrene-edge type" (or armchair edge type), which present different electronic properties.[7–10] The *n*-acenes molecules (composed of *n* edge-fused aromatic rings, such as benzene, naphthalene, antracene, tetracene, and pentacene) have attracted great interest not only for their electronic structure (see, e.g., Refs. 11 and 12 and references quoted therein) but also for practical applications in thin-film transistors[13,14] as electrodes for lithium ion batteries[15,16] and in molecular electronics.[17]

Although *n*-acenes with only up to seven rings have been synthesized,[18] the ground and excitation electronic properties of the infinite one-dimensional hypothetical polyacene polymer $[(C_4H_2)_n]$ have been widely studied since the seminal paper of Kivelson and Chapman.[19] Polyacene resembles two interacting polyacetylene $[(CH)_n]$ chains; as well, zigzag graphene nanoribbons can be considered as composed of parallel undistorted polyacetylene chains cross-linked together (see Fig. 1). Two central issues have been addressed with different theoretical methods in the study of electronic structure of polyacenes: the Peierls distortion[19,20] due to electron-phonon interaction and the role of electron-electron interaction.[21–24] Theoretical investigations have also been devoted to the structural and electronic properties of large aromatic hydrocarbons as models for two-dimensional graphite[25,26] a topic highlighted in the original papers of Longuet-Higgins and Salem[27] and of Anno and Coulson.[28] Recently, the effect of disorder on electron transmission of polyacene chains has been evaluated in analogy with transport in ultranarrow graphene nanoribbons.[29]

The purpose of the present paper is to investigate the transport properties of gated conjugated polymers of the polyacene series, composed of a small number *N* of chains, as well as of ultranarrow zigzag graphene ribbons. Our simulations demonstrate that the polymeric system is insulating or conducting according to the Fermi energy of the injected electrons, of the even or odd number of chains, and of the shape of the gate potential. The numerical simulations are performed for nondistorted polymeric structures with lowest conduction and highest valence bands touching at the border of the Brillouin zone.

In Sec. II we consider the electronic structure of polymers of the polyacene family and we focus on the features determined by the symmetry and by the lattice honeycomb topology. In Sec. III we present numerical simulations of the conductance of gated polyacenes as a function of relevant parameters, such as the gate potential, the Fermi energy of carriers, and the number of composing chains. In this section we also report a detailed analysis of the effects of spatial symmetry and lattice topology on the interband scattering. Field-effect control of metallic and insulating regimes was originally investigated in wide graphene ribbons and connected to the double valley structure around the two Dirac points[30,31] and to the system symmetry.[32] We show here that field-effect control of resistance is also operative in polyacenes, being essentially related to the lattice symmetry. Section IV contains the conclusions.

II. ELECTRONIC BAND STRUCTURE OF UNDISTORTED POLYACENES

The geometrical configuration of polymers of the polyacene series with chosen even or odd values *N* of zigzag chains is reported in Fig. 1. All polymers of the polyacene series are arranged in one-dimensional lattices with D_{2h} as point group. It can be seen by inspection that upper and lower edges in the ribbons with odd *N* exhibit a zigzag configuration shifted in the *x* direction by the fractional translation $f=a/2$, where *a* is the lattice constant. As a consequence, for odd *N* the spatial group of the ribbons is nonsymmorphic[33,34] with half operations of the point group D_{2h} associated with fractional translations. In particular the mirror reflection symmetry with respect to a plane perpen-

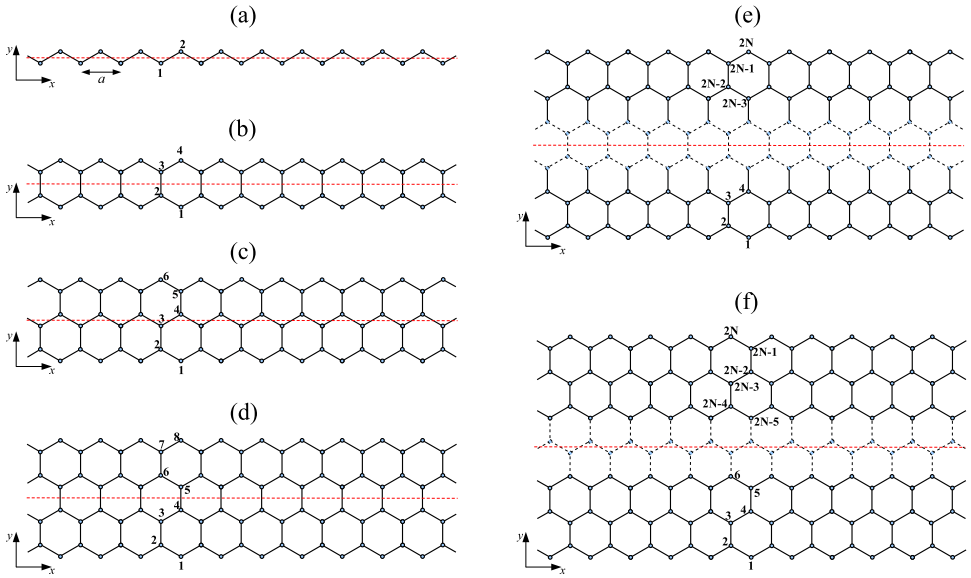

FIG. 1. (Color online) Undistorted lattice structures of (a) polyacetylene, $N=1$, (b) polyacene, $N=2$, (c) polyacenacene, $N=3$, (d) polyperylene, $N=4$, (e) generic ribbon with even number N of zigzag chains, and (f) generic ribbons with odd N. Numbering of the $2N$ sites of the primitive cell of the polyacene series is also shown. When N is even, the lattice is invariant under reflections with respect to the orthogonal plane indicated by the broken horizontal lines. If N is odd, the mirror reflection must be followed by a fractional translation of $a/2$ along the x axis.

dicular to the polymer plane and bisecting the central rung bonds is associated with fractional translations for odd N and ordinary integer translations for even N. These considerations (complemented by standard symmetry analysis[33,34]) are shown to be at the heart of the *even-odd effect* in electronic transport: This effect was originally observed in wide graphene ribbons,[30–32] whose band structures carry an evident reminiscence of the two Dirac points of graphene, and for this reason it was referred to as *valley filter effect*. It is shown below that the even-odd effect is a robust consequence of symmetry, and as such it occurs also in ultranarrow ribbons, including the extreme situation of $N=2$, where no reminiscence of Dirac points occurs in the band structure. The purpose of this section is to highlight the consequences of symmetry and topology on the electronic band structure of polyacene polymers.

A generic undistorted graphene ribbons with N chains is translationally invariant along the longitudinal x axis. The independent sites in the primitive cell are numbered as in Fig. 1. From the p_z carbon orbitals of the ribbon and for each site d_j $(j=1,2,\ldots,2N)$ within the unit cell, we form the Bloch sums,

$$\Phi_j(k_x) = \frac{1}{\sqrt{M}} \sum_m e^{ik_x(t_m+d_{jx})} \phi_{mj} \quad j=1,2,\ldots,2N, \qquad (1)$$

with $t_m=ma$, a is the lattice constant, d_{jx} denotes the x component of the position vectors in the primitive cell, and M is the (arbitrarily large) number of primitive cells. We adopt a nearest-neighbor tight-binding description of the p_z dangling carbon orbitals of the undistorted polymer in the basis set of Bloch functions [Eq. (1)]. The diagonal matrix elements are taken all as equal to zero, and the off-diagonal matrix elements are different from zero only between consecutive Bloch functions and are given alternatively by $2t\cos(k_xa/2)$ and t, where t is the nearest-neighbor interaction (hopping parameters between nearest-neighbor carbon dangling orbitals are negative with typical values of the order of electron volt). In the following, $|t|$ is taken as unit of energy and the site energy of the dangling orbitals is taken as the reference energy and set equal to zero. The Hamiltonian of a ribbon with N zigzag chains in the k representation takes the tridiagonal form,

$$H(k_x) = \begin{bmatrix} 0 & 2tc(k_x) & 0 & 0 & 0 & 0 & \cdots \\ 2tc(k_x) & 0 & t & 0 & 0 & 0 & \cdots \\ 0 & t & 0 & 2tc(k_x) & 0 & 0 & \cdots \\ 0 & 0 & 2tc(k_x) & 0 & t & 0 & \cdots \\ 0 & 0 & 0 & t & 0 & 2tc(k_x) & \cdots \\ 0 & 0 & 0 & 0 & 2tc(k_x) & 0 & \cdots \\ \cdots & \cdots & \cdots & \cdots & \cdots & \cdots & \cdots \end{bmatrix}_{2N}, \qquad (2)$$

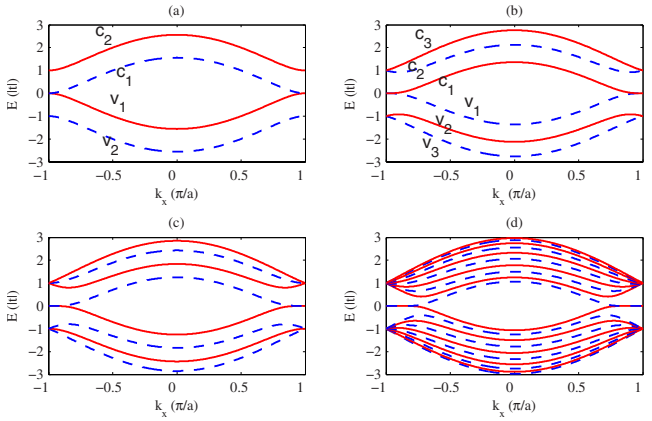

FIG. 2. (Color online) Energy bands of clean undistorted wires of (a) polyacene, $N=2$, (b) polyacenacene, $N=3$, (c) polyperylene, $N=4$, and (d) of a ribbon with $N=10$ zigzag chains. For N even, the eigenstates have definite parity with respect to the mirror symmetry operation. Those on the dashed blue bands are even and those on the continuous red bands are odd. For N odd, the eigenstates have definite parity with respect to the glide plane symmetry operation. Those on the dashed blue bands are even and those on the continuous red bands are odd.

where $c(k_x)=\cos(k_x a/2)$; the diagonalization of $H(k_x)$ gives the electronic band structure of the ribbon. Notice that the eigenvalues of the matrix [Eq. (2)] at $k_x=\pm\pi/a$ are

$$E=0(\text{twofold degenerate})$$

and

$$E=+|t|;-|t|(N-1-\text{fold degenerate}).$$

From the form of matrix (2) and the corresponding band structures reported in Fig. 2, the following features can be evidenced: (i) electron-hole symmetry of the spectrum for positive and negative energy values, (ii) degeneracy at the border of the Brillouin zone of the top valence band and the bottom conduction band, whose wave functions are confined at the two spatial edges for $k=\pm\pi/a$, (iii) degeneracy ($N-1$ times) of the upper group of energy bands with energy $|t|$ at the border of the Brillouin zone and similar behavior of the lower group of energy bands with energy $-|t|$, and (iv) development of two tendentially dispersionless energy bands at the reference energy zero (covering over one-third of the Brillouin zone for large N and already evident also for $N=10$). In summary, the honeycomb topology of the undistorted polymeric ribbons give rise to three groups of band (see Fig. 2): a lower group of $N-1$ holelike bands indicated by $[v_2,v_3,\ldots,v_N]$, a central group that consists of the highest valence band v_1 and the lowest conduction band c_1, and the upper group of $N-1$ electronlike bands indicated by $[c_2,c_3,\ldots,c_N]$. Each group of bands is degenerate at the borders of the Brillouin zone ($k_x=\pm\pi/a$).

The energy bands of the polymeric ribbons, obtained from Hamiltonian (2), can be classified as even or odd according to the symmetry of their eigenvectors. Parity is even for the bottom conduction band c_1 and odd for the top valence band v_1 if N is even. The opposite occurs if N is odd. Adjacent

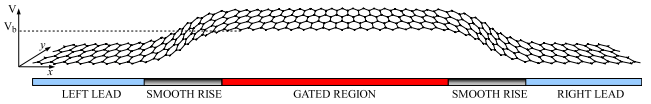

FIG. 3. (Color online) Schematic representation of the potential barrier induced by the gate. The potential rises smoothly from zero in the left and right lead regions to the value V_b in the gated region.

energy bands have opposite parities. Although we only consider nearest-neighbor interactions, it should be noticed that the presence of second-nearest-neighbor interactions or higher-order interactions does not affect the symmetry of the lattice.

We consider now the effects of a superimposed gate potential on the crystalline wave functions. In general, when defects are introduced, spatial symmetries are broken. However, if the defect under attention is a superimposed gate potential independent of the transverse coordinate, mirror reflection symmetry is preserved in even ribbons regardless how sharp or smooth is the shape of the superimposed potential. In fact, a gate potential that only depends on the longitudinal coordinate x (see Fig. 3) can be represented in the form

$$V_{\text{gate}}=\sum_{mj} V_m|\phi_{mj}\rangle\langle\phi_{mj}|, \tag{3}$$

where m is the cell index and j runs over the $2N$ sites of each unit cell. It is important to notice that for ribbons that are composed of an even number N of chains, the potential gate in Eq. (3) is invariant under the lattice mirror operation. If N is odd, V_{gate} is not invariant under the lattice glide plane symmetry operation. Thus, for even N the gate potential does not couple bands of opposite parity, and transport channels of different parity remain unmixed and mutually independent.

Besides the symmetry of the gate potential, its shape may also affect interband scattering. In fact, let us consider the matrix elements of V_{gate} between two eigenfunctions of the type

$$|\Psi_\alpha(k)\rangle=\sum_j c_j^{(\alpha)}|\Phi_j(k)\rangle,$$

where α is the band index and $|\Phi_j\rangle$ are given in Eq. (1). We have

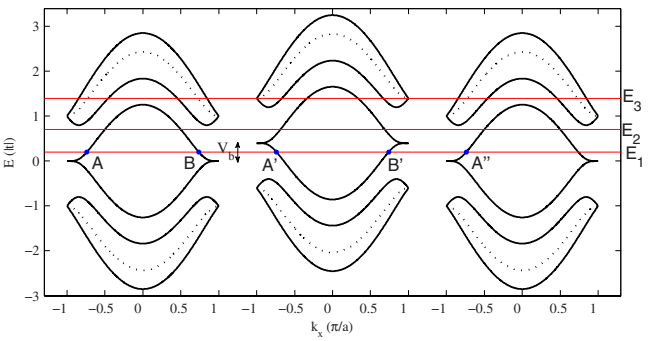

FIG. 4. (Color online) Schematic band structure of the polyacene ribbon in the left lead, gated region, and right lead. In the central gated region, the bands are shifted by the gate potential V_b.

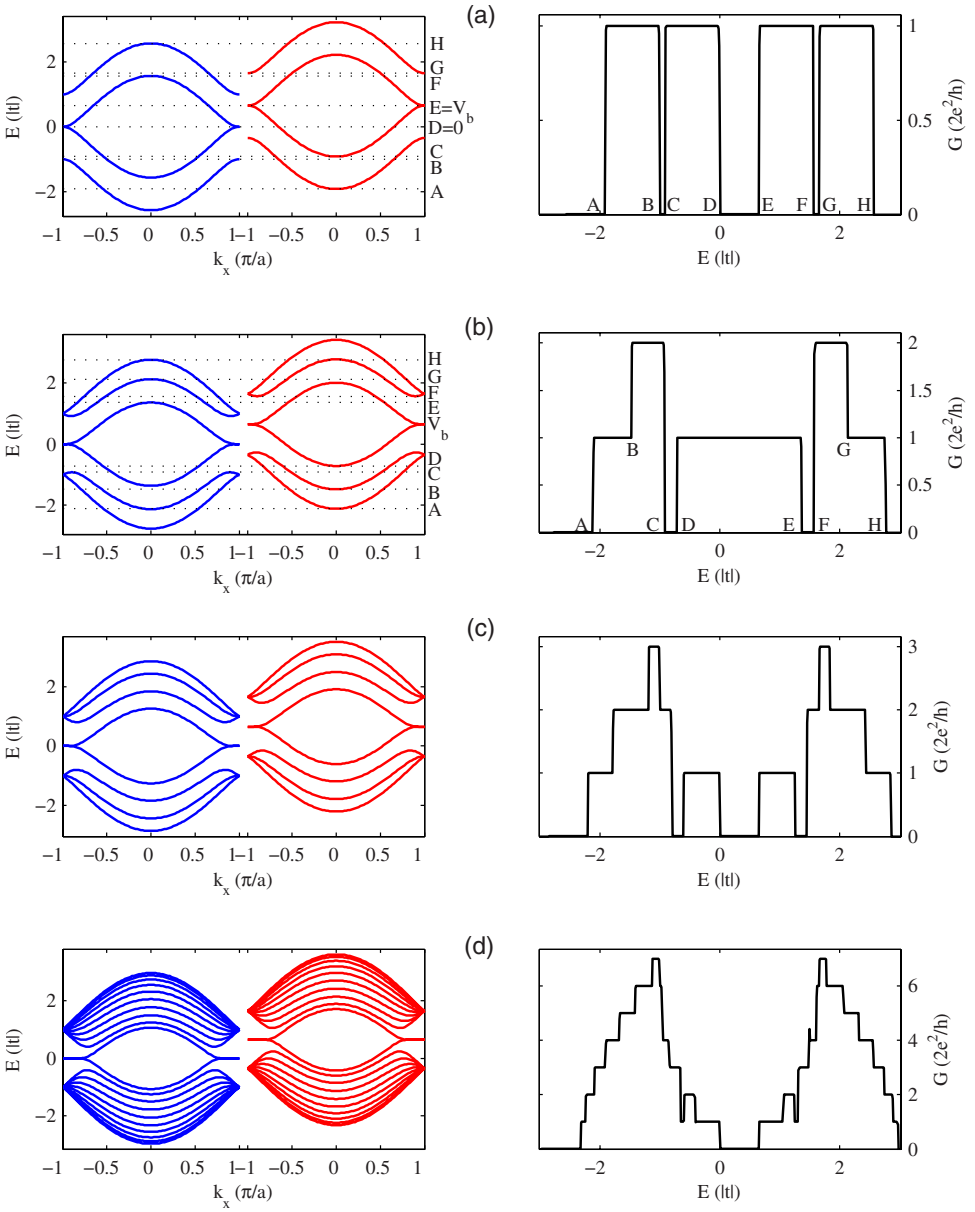

FIG. 5. (Color online) Energy bands (of the left lead and of the central gated region) and conductances of (a) polyacene, $N=2$, (b) polyacenacene, $N=3$, (c) polyperylene, $N=4$, and (d) ribbon composed of $N=10$ chains. The value of the applied smooth gate potential is $V_b=0.65|t|$.

$$\langle \Psi_\alpha(k)|V_{\text{gate}}|\Psi_\beta(q)\rangle = \sum_{jj'} c_j^{(\alpha)*}(k)c_{j'}^{(\beta)}(q)\langle \Phi_j(k)|V_{\text{gate}}|\Phi_{j'}(q)\rangle$$

$$= \sum_{jj'} c_j^{(\alpha)*}(k)c_{j'}^{(\beta)}(q)\,\delta_{jj'}e^{-i(k-q)d_{jx}}\frac{1}{M}\sum_m V_m e^{-i(k-q)t_m}$$

$$= \sum_j c_j^{(\alpha)*}(k)c_j^{(\beta)}(q)e^{-i(k-q)d_{jx}}V_{\text{gate}}(k-q), \qquad (4)$$

where $V_{\text{gate}}(k-q)$ denotes the Fourier transform of the gate potential. The Fourier transform of V_{gate} is significant for $|k-q|$ up to values of the order of the inverse of the length of the region where the gate potential varies (see Fig. 3). Therefore, spatially smooth potentials can only scatter an electron into states with continuously varying k values. As a consequence, such a potential can adiabatically guide electron states along the same band or along other related bands with common degeneracy points.

III. CHARGE TRANSPORT IN POLYMERIC CHAINS

In this section, we consider the conductance of polyacene ribbons of Fig. 1 with a superimposed smooth potential barrier of the shape indicated in Fig. 3 for various values of the barrier height V_b. The numerical evaluation of the differential conductance of zigzag nanoribbons is performed with the Keldysh formalism,[35,36] appropriately implemented for the honeycomb lattice topology.[37,38]

For a large gated region, the energy spectrum in the leads and in the gated region can be represented, as shown in Fig. 4, for the case of a generic undistorted polymer of the polyacene family. The energy bands of the gated region are shifted by the value V_b. From Fig. 4 we can also infer the qualitative behavior of an electron injected, e.g., from the left lead at a chosen energy E. If $0<E_1<V_b$ the electron is injected from the left lead in channel A and then enters the gated region in channel A′ or is reflected in channel B. Eventually, it can be transmitted to channel A″ of the right

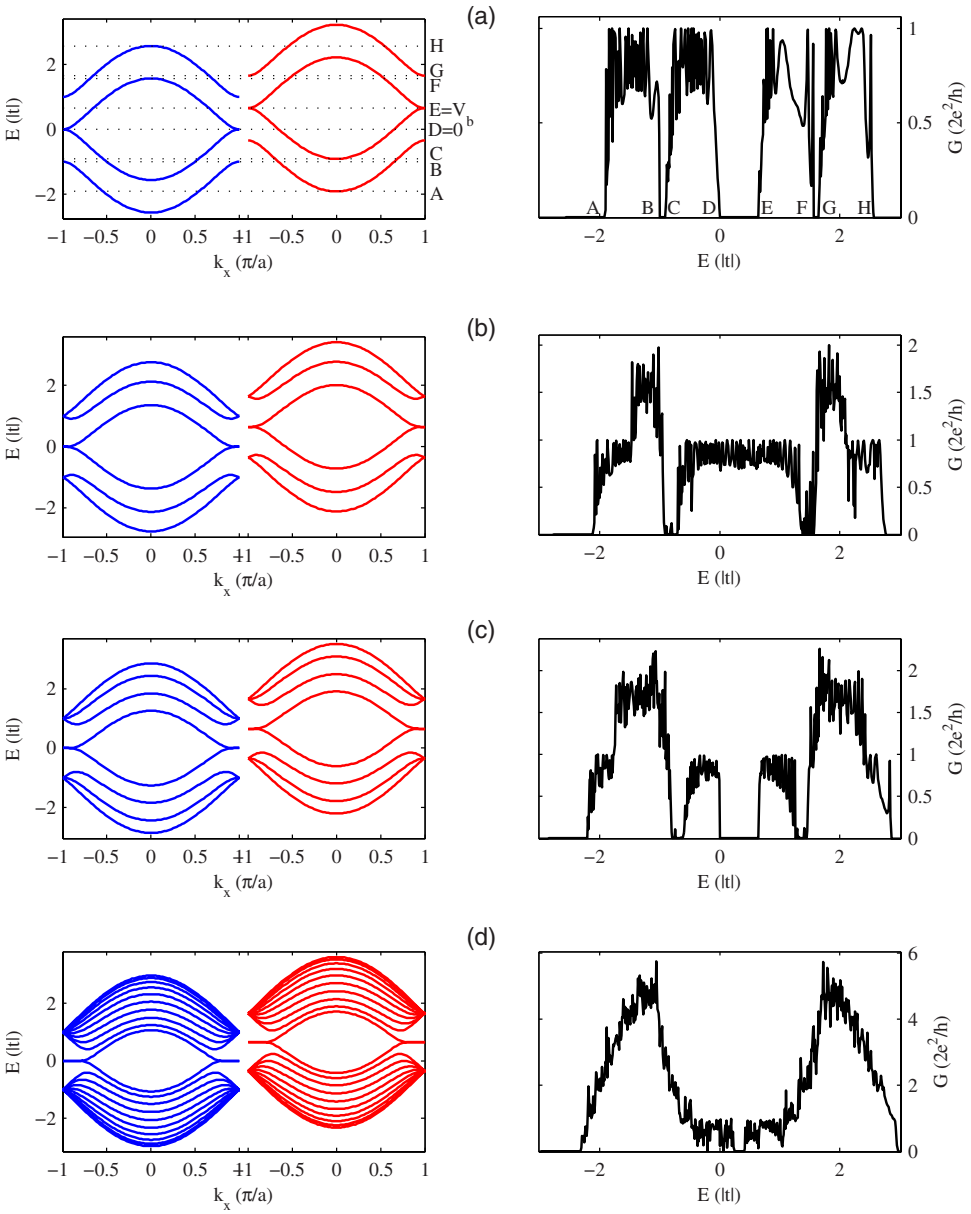

FIG. 6. (Color online) Energy bands (of the left lead and of the central gated region) and conductances of (a) polyacene, $N=2$, (b) polyacenacene, $N=3$, (c) polyperylene, $N=4$, and (d)ribbon composed of $N=10$ chains. The value of the applied sharp gate potential is $V_b=0.65|t|$.

lead or reflected into channel B′. Notice that the electron lies in the bottom conduction band in the lead regions and in the topmost valence band in the gated regions. Since these bands have opposite parity under the symmetry group of the ribbon, the electron transmission is only possible for odd number of chains, and thus, at the chosen energy, only polymers composed of an odd number of chains are conducting.

With similar reasoning we can analyze electrons injected at the energy $E_2 > V_b$, where a single band is active in each region (see Fig. 4). In this case transmission is possible for polymers with both even and odd number of chains.

In the case in which the energy of the injected electron, E_3, encounters several bands (see Fig. 4), scattering is allowed between states with the same parity if N is even. However, as discussed in Sec. II, due to the smoothness of the superimposed potential, an electron changes its momentum continuously while entering or exiting the gated central region. Thus, no scattering occurs between states belonging to different groups of bands (upper, central, and lower) since the electron cannot pass from one group of bands to another continuously. For the same reason, scattering is allowed between states belonging to the same group of bands. In this case, we expect quantization of the conductance because backscattering is efficiently suppressed in the presence of smooth potentials. On the contrary, scattering between different groups of bands is possible in the case of sharp profile of the gate potential due to the high momentum components of its Fourier transform [see Eq. (4)].

The above considerations are verified by our numerical calculations reported in Fig. 5 for polymer ribbons composed of $N=2$, 3, 4, and 10 carbon chains, with a superimposed gate potential $V_b=0.65|t|$. The regions where the potential rises extend over 200 primitive cells. In Fig. 5, we report the band structures (left panels) and the differential conductances G (right panels) evaluated for the considered ribbons. Since the band structure in the left lead is the same as in the right lead (see Fig. 4), we only show the energy bands of the left lead and of the gated region.

In the case of polyacene ($N=2$), the energy regions where the system is perfectly conducting or insulating, see Fig. 5(a), are easily interpreted in terms of the electronic bands structure. In fact, it holds $G=0$ below the energy A because no states are available in the gated region. In the interval A–B the band v_2 is active through the whole system, while the band v_1 may be active in the leads regions. In each region, v_1 and v_2 have opposite parity and belong to different groups of bands. Thus, the electrons injected in the band v_2 are perfectly transmitted, while those injected in the band v_1 are fully backscattered. This justifies the value $G=2e^2/h$ in the energy interval A–B. In the energy range B–C, $G=0$ because only bands v_1 are active in the leads, while only the band v_2 is active in the gated region. For energies in interval C–D, we have $G=2e^2/h$, in fact only the bands v_1 are active in both the leads and the gated regions. The value $G=0$ in interval $D=0-E=V_b$ is motivated by the different parity of the bands c_1 in the leads and the band v_1 in the gated region. A specular behavior is observed in the higher energy intervals E–F, F–G, and G–H.

In the case of polyacenacene, reported in Fig. 5(b), the number of chains is odd and thus the scattering between states belonging to bands with opposite parity is allowed. In fact, we observe that the polymeric ribbon is conducting in the energy range $0-V_b$, where the bands c_1 are active in the leads, while the band v_1 is active in the gated region. The value $G=0$ in the energy intervals C–D and E–F of Fig. 5(b) is due to the fact that in the leads and in the gated region the states belong to different groups of bands.

Similarly, the even/odd effect and the considerations concerning to the honeycomb lattice topology of the system can be exploited to interpret ribbons composed of higher number of chains as reported in Fig. 5(c) (for $N=4$) and Fig. 5(d) (for $N=10$).

In Fig. 6, we consider the same systems in the presence of a steep rise of the potential barrier. In contrast to the case of smooth potential, the wave vector of the injected particles can now vary discontinuously. This entails two main consequences: First, the conductance is no more quantized due to the enhanced backscattering even if a reminiscence of the plateaus is still evident. Moreover, the scattering between different groups of bands is now allowed. Let us consider the case of polyacene [Fig. 6(a)]. We can clearly see that the gaps among the points B–C, D–E, and F–G are still present. In fact transmission is forbidden in these energy ranges due to the different parity of the states in the leads and in the gated region. In the case of polyacenacene, reported in Fig. 6(b), the gaps we had for the smooth potential are no more present. Due to the possibility of intergroup scattering, small transmission is allowed. These effects are more evident for the polyperylene [see Fig. 6(c)]. In this case, the gap in the conductance close to the neutrality point is still preserved because it is due to symmetry reasons, while the transmission is different from zero in correspondence of the other two gaps because the possibility of scattering between different groups of bands.

In summary, we notice explicitly that for appropriate energy intervals to the right of the reference energy $E=0$, all even ribbons are perfectly insulating (see Figs. 5 and 6 and the previous discussion). This behavior, appealing for electronic valve applications, was first observed for wide graphene ribbons.[30,31] It occurs regardless of the two-valley band structure of graphene and also holds for ultranarrow graphene ribbons. We have in fact shown that the origins of the effect are symmetry and topology. It is also worthwhile to notice that the useful energy interval for electronic valve control is of the order of $|t|/N$ (approximately equal to hundredths of electron volt) around $E=0$ for typically wide graphene ribbons, while it is of the order of $|t|(\approx$ eV) for polyacene and ultranarrow materials.

IV. CONCLUSIONS

We have calculated the conductance of gated polymers of the polyacene family within a tight-binding representation of the π electron Hamiltonian and the nonequilibrium Keldysh formalism. The transport properties have been studied as a function of the even or odd number of chains composing the ribbons and of the energy of the injected carriers in the presence of gate potentials with smooth and sharp stepwise profiles, depending only on the longitudinal coordinate. The numerical simulations indicate that gate voltages can efficiently block the current flow in the even mesoscopic systems. We have seen in fact that in the case of an even number of chains the blocking of current (in the energy range where a single electronlike or holelike energy channel is active) is a robust effect, essentially related to spatial symmetry and ribbon topology.

ACKNOWLEDGMENTS

This work was supported by Scuola Normale Superiore and by National Enterprise for Nanoscience and Nanotechnology (NEST).

[1] T. Seideman, J. Phys.: Condens. Matter **15**, R521 (2003).
[2] J. V. Barth, G. Costantini, and K. Kern, Nature (London) **437**, 671 (2005).
[3] A. Nitzan and M. A. Ratner, Science **300**, 1384 (2003).
[4] M. Di Ventra, S. T. Pantelides, and N. D. Lang, Phys. Rev. Lett. **84**, 979 (2000).
[5] J.-C. Charlier, X. Blase, and S. Roche, Rev. Mod. Phys. **79**, 677 (2007).
[6] J. Nilsson, A. H. Castro Neto, F. Guinea, and N. M. R. Peres, Phys. Rev. B **78**, 045405 (2008).
[7] D. Prezzi, D. Varsano, A. Ruini, A. Marini, and E. Molinari, Phys. Status Solidi B **244**, 4124 (2007).
[8] K. Yoshizawa, K. Yahara, K. Tanaka, and T. Yamabe, J. Phys. Chem. B **102**, 498 (1998).
[9] M. Ezawa, Phys. Rev. B **73**, 045432 (2006).
[10] V. Barone, O. Hod, and G. E. Scuseria, Nano Lett. **6**, 2748

(2006).
[11] De-en Jiang and Sheng Dai, J. Phys. Chem. A **112**, 332 (2008).
[12] M. C. dos Santos, Phys. Rev. B **74**, 045426 (2006).
[13] M. Bedmikov, F. Wude, and D. F. Pepepichka, Chem. Rev. (Washington, D.C.) **104**, 4891 (2004).
[14] M. Halik, H. Klauk, U. Zschieschang, G. Schmid, C. Dehm, M. Schütz, S. Maisch, F. Effenberger, M. Brunnbauer, and F. Stellacci, Nature (London) **431**, 963 (2004).
[15] T. Zheng, J. S. Xue, and J. R. Dahn, Chem. Mater. **8**, 389 (1996).
[16] G. Madjarova and T. Yamabe, J. Phys. Chem. B **105**, 2534 (2001).
[17] M. E. Gershenson, V. Podzorov, and A. F. Morpurgo, Rev. Mod. Phys. **78**, 973 (2006).
[18] E. Clar, *Polycyclic Hydrocarbons* (Academic, London, 1964), Vols. 1 and 2.
[19] S. Kivelson and O. L. Chapman, Phys. Rev. B **28**, 7236 (1983).
[20] I. Bozović, Phys. Rev. B **32**, 8136 (1985).
[21] A. L. S. da Rosa and C. P. de Melo, Phys. Rev. B **38**, 5430 (1988).
[22] C. Raghu, Y. Anusooya Pati, and S. Ramasesha, Phys. Rev. B **65**, 155204 (2002).
[23] B. Srinivasan and S. Ramasesha, Phys. Rev. B **57**, 8927 (1998).
[24] M. P. O'Connor and R. J. Watts-Tobin, J. Phys. C **21**, 825 (1988).
[25] N. Tyutyulkov, K. Müllen, M. Baumgarten, A. Ivanova, and A. Tadjer, Synth. Met. **139**, 99 (2003).
[26] N. Tyutyulkov, G. Madjarova, F. Dietz, and K. Müllen, J. Phys. Chem. B **102**, 10183 (1998).
[27] H. C. Longuet-Higgins and L. Salem, Proc. R. Soc. London, Ser. A **257**, 445 (1960).
[28] T. Anno and A. Coulson, Proc. R. Soc. London, Ser. A **264**, 165 (1961).
[29] N. M. R. Peres and F. Sols, J. Phys.: Condens. Matter **20**, 255207 (2008).
[30] A. Rycerz, J. Tworzydlo, and C. W. J. Beenakker, Nat. Phys. **3**, 172 (2007).
[31] A. R. Akhmerov, J. H. Bardarson, A. Rycerz, and C. W. J. Beenakker, Phys. Rev. B **77**, 205416 (2008).
[32] A. Cresti, G. Grosso, and G. Pastori Parravicini, Phys. Rev. B **77**, 233402 (2008).
[33] G. F. Koster, in *Solid State Physics*, edited by F. Seitz and D. Turnbull (Academic, New York, 1957), Vol. 5, p. 173.
[34] F. Bassani and G. Pastori Parravicini, *Electronic States and Optical Transitions in Solids* (Pergamon, Oxford, 1975).
[35] D. K. Ferry and S. M. Goodnick, *Transport in Nanostructures* (Cambridge University Press, Cambridge, England, 1997).
[36] R. Lake, G. Klimeck, R. Brown, and D. Jovanovich, J. Appl. Phys. **81**, 7845 (1997).
[37] A. Cresti, G. Grosso, and G. Pastori Parravicini, Phys. Rev. B **76**, 205433 (2007).
[38] L. P. Zârbo and B. K. Nikolić, Europhys. Lett. **80**, 47001 (2007).